

Multimodal Bioactivation of Hydrophilic Electrospun Nanofibers Enables Simultaneous Tuning of Cell Adhesivity and Immunomodulatory Effects

Laura Wistlich, Juliane Kums, Angela Rossi, Karl-Heinz Heffels, Harald Wajant, and Jürgen Groll*

Biomaterials research usually focuses on functional and structural mimicry of the extracellular matrix or tissue hierarchy and morphology. Most recently, material-induced modulatory effects on the immune system to arouse a healing response is another upcoming strategy. Approaches, however, that integrate both aspects to induce healing and facilitate specific cell adhesion are so far little explored. This study exploits manifold but chemical crosslinker free functionalization of hydrophilic and nonadhesive electrospun fiber surfaces with peptides for controlled cell adhesion, and with neutralizing antibodies targeting the master cytokine tumor necrosis factor (TNF) to dampen proinflammatory reactions by the fiber adherent cells. It is demonstrated that cell attachment and immunomodulatory properties of a textile can be tailored at the same time to generate meshes that combine immunosuppressive activity with specific cell adhesion properties.

1. Introduction

Electrospinning is a simple method to produce nonwoven meshes composed of micrometer- to nanometer-sized fibers^[1] with versatile applicability, including filtration,^[2] sensing,^[3] and textiles.^[4] Since such scaffolds can be tailored to resemble a close similarity to the fibrous extracellular matrix in connective tissue,^[5] their application in biomaterials research and tissue engineering has been on particular focus.^[6] Biodegradable synthetic polymers like the often used polyesters poly(lactic-co-glycolic acid)

(PLGA) or polycaprolactone (PCL) are usually hydrophobic,^[7] such that uncontrolled protein adsorption is the primary step of interaction with biology, which subsequently leads to cell attachment and proliferation on such scaffolds.^[8] Numerous attempts have thus been undertaken to generate a more rapid and especially more specific cell adhesion through improvement of the scaffolds' surface chemistry. However, many published methods are mainly based on multistep postprocessing procedures.^[9] A transformation of the hydrophobic fiber surface into hydrophilic material is commonly achieved via surface graft polymerization which needs several functionalization steps.^[10] Recent studies demonstrated *in situ* functionalization

of PCL microfibers by spinning them directly in a coagulation bath collector filled with polydopamine.^[11] These fibers were then used for differentiation studies of human mesenchymal stem cells. Nicolini et al. functionalized PCL nanofibers with particles bearing carboxyl or amine groups for further functionalization working with reverse potential spinning mode.^[12] Furthermore, they exploited these particles for immobilization with the sequence arginyl-glycyl-aspartic acid (RGD) to increase human umbilical vein endothelial cell attachment. Another study dealt with self-assembly of diblock copolymers at the solid-air interface of poly(DL-lactide) electrospun fibers to enhance the hydrophilicity; an RGD sequence was introduced here by thiol-ene interaction.^[13]


An alternative approach is the use of hydrophilic additives that segregate to the surface during the spinning process. One example is the application of six-armed, star-shaped, polyethylene glycol (PEG)-based prepolymers with reactive isocyanate (NCO) groups at the distal endings of the polymer arms (NCO-sP(EO-*stat*-PO)) as additive for the electrospinning of PLGA. This strategy results in hydrophilic fibers directly after spinning, where the PEG content minimizes protein adsorption and cell adhesion, and the isocyanates remain as an anchor for straightforward but versatile functionalization possibilities with peptides for cell attachment.^[14]

In case a therapeutic application is envisioned, it is important to appreciate the initial immune reaction of the host to the material after implantation that in the worst-case scenario may lead to foreign body reaction. Accordingly, the implementation

L. Wistlich, Dr. A. Rossi, Dr. K.-H. Heffels, Prof. J. Groll
Department for Functional Materials in Medicine and Dentistry
and Bavarian Polymer Institute (BPI)
University of Würzburg
Pleicherwall 2, 97070 Würzburg, Germany
E-mail: juergen.groll@fmz.uni-wuerzburg.de

Dr. J. Kums, Prof. H. Wajant
Department of Internal Medicine II
Division of Molecular Internal Medicine
University Hospital Würzburg
Röntgenring 11, 97070 Würzburg, Germany

Dr. A. Rossi
Department of Tissue Engineering and Regenerative Medicine
University of Würzburg
Röntgenring 11, 97070 Würzburg, Germany

 The ORCID identification number(s) for the author(s) of this article can be found under <https://doi.org/10.1002/adfm.201702903>.

DOI: 10.1002/adfm.201702903

of immunosuppressive properties into biomaterials has recently gained attention.^[15] Different strategies are pursued to achieve this goal that comprise immunomodulatory effects of 3D morphology of materials^[16] and adjusting the surface chemistry.^[17] However, few studies so far aim at integrating immunomodulatory effects for the early phase after implantation and specific interaction with cells that are responsible for tissue remodeling and regeneration, such as resident stem cells and tissue cells.

Here, we present a method for a multimodal functionalization of polymeric and hydrophilic nanofiber meshes to combine immune-regulatory properties with specific cell adhesion. We demonstrate based on fluorescence that threefold functionalization can be achieved using NCO-sP(EO-*stat*-PO) as additive. We exploit this by immobilizing cell-adhesion-mediating RGD peptides in a first functionalization step through prefabrication addition of the peptide into the spinning solution, followed by a second functionalization step in which different proteins for immunomodulation were immobilized using the active isocyanate groups on the surface of freshly prepared fibers. The first protein was a human neutralizing monoclonal antibody against tumor necrosis factor α (TNF), which inhibits TNF binding to its receptor.^[18] The second protein was 5B6, a recombinant antibody against fibroblast growth-factor-inducible 14 molecule (Fn14) which has been implicated in a variety of tissue-damage-associated complications.^[19] Binding studies showed that the antibodies were immobilized successfully. Cell culture experiments demonstrate that we could tune cell adhesion and, at the same time but independent thereof, were able to influence cell activity and inflammation processes, which are important in foreign body reaction.

2. Results and Discussion

It is challenging to functionalize the surface of textiles, especially nanofibrous meshes, in order to control biological behavior of cells and the way a biomaterial interacts with the body. In literature, two different chemical functionalization routes are described for solution electrospinning. First, biological molecules can be added before the procedure, for example, by bulk modification of used polymers^[20] or by including the peptides directly in the spinning solution.^[14a] The second possible method is the surface modification postspinning, for instance, by coating of spun fibers with a solution of the biological additive.^[21] The purpose of the current study was the examination of realizing a multimodal functionalization of electrospun meshes prepared out of PLGA and the functional additive NCO-sP(EO-*stat*-PO) comprising both of the mentioned functionalization approaches in a consecutive manner without the need for additional chemical crosslinking agents. To achieve this, at first the multimodal fiber functionalization was established, then transferred to the immobilization of bioactive molecules, and finally assessed by cell culture tests.

2.1. Crosslinker Free Multimodal Functionalization of Electrospun Fibers

Electrospinning of polyesters with the star-shaped prepolymer NCO-sP(EO-*stat*-PO) as functional component leads to

hydrophilic fibers due to surface segregation of the hydrophilic additive during spinning.^[14a] Beyond that, the isocyanate groups of NCO-sP(EO-*stat*-PO) open various possibilities to modify the fiber surface with bioactive molecules if these bear protic groups such as amines or thiols for covalent binding to the isocyanates. These molecules can be added to the spinning solution, so that coupling to NCO-sP(EO-*stat*-PO) occurs in solution and both moieties segregate to the surface together.^[14a,22] This strategy is, however, limited to molecules which are compatible with the solution of the hydrophobic polyester that is used for the spinning procedure; this significantly narrows the variety of introducible molecules.

Here, we extend the fiber surface functionalization with incubation steps in aqueous solutions to covalently bind either protic or amino-reactive molecules to the fiber surface. **Figure 1A** displays the simplicity of the resulting threefold functionalization protocol. Since the fibers have a very low intrinsic green and no red fluorescence (Figure S1, Supporting Information), a green and a red dye were chosen as model molecules for the functionalization studies. First step is the known addition of a molecule with isocyanate reactive groups such as thiols, amines, or hydroxyl groups (e.g., present in RGD, biocytin) into the electrospinning solution, which was done here by adding biocytin. Exposed on the fiber surface, biocytin can be linked to streptavidin (SA) forming a strong noncovalent bond.^[23] Here, green fluorescent SA-coated polystyrene beads were added for visualization as we are interested in functional groups on the electrospun fiber surface. In Figure S2 in the Supporting Information, several beads were observable which are fixed on the top and on the side of biocytin containing fibers. Control studies revealed no unspecific attachment of SA beads, hence the results suggest a surface-active presence of biocytin (Figure S3, Supporting Information).

After fiber spinning, one or more additional NCO-sensitive substances can be attached to unreacted isocyanate groups on the freshly spun fiber surface by immersing the mesh in an aqueous solution of the reactive molecule. Here, the fibrous samples were incubated in a solution of 0.05 mg mL⁻¹ Alexa Fluor 568 cadaverine. The fluorescent micrographs revealed a red fluorescence of the postspinning dyed fibers in contrast to untreated fibers (Figure 1B). Irrespective of the described pretreatments, any remaining isocyanate will be hydrolyzed in water or by air humidity and is available as amine for further functionalization.^[24] The third possibility is thus accessible by incubation with amine reactive molecules such as active esters. Our model reaction contained the green fluorescent dye Alexa Fluor 488 with a succinimidyl residue. The active ester-amine reaction took place in an aqueous solution of 0.05 mg mL⁻¹ Alexa Fluor 488 N-hydroxysuccinimide (NHS) ester within 2 h. The immobilization was investigated with fluorescence imaging showing a strong green fluorescence, which indicated the successful reaction (Figure S4, Supporting Information).

Besides the presented single functionalization any two combinations as well as a threefold functionalization can be generated as demonstrated in Figure 1B for the same spot of mesh: The green fluorescent SA-coated PS beads that attach to biocytin, the red fluorescence of the amino-functional dye that binds to the NCO groups and the green fluorescence of the fiber which was introduced by reaction of the amino-reactive

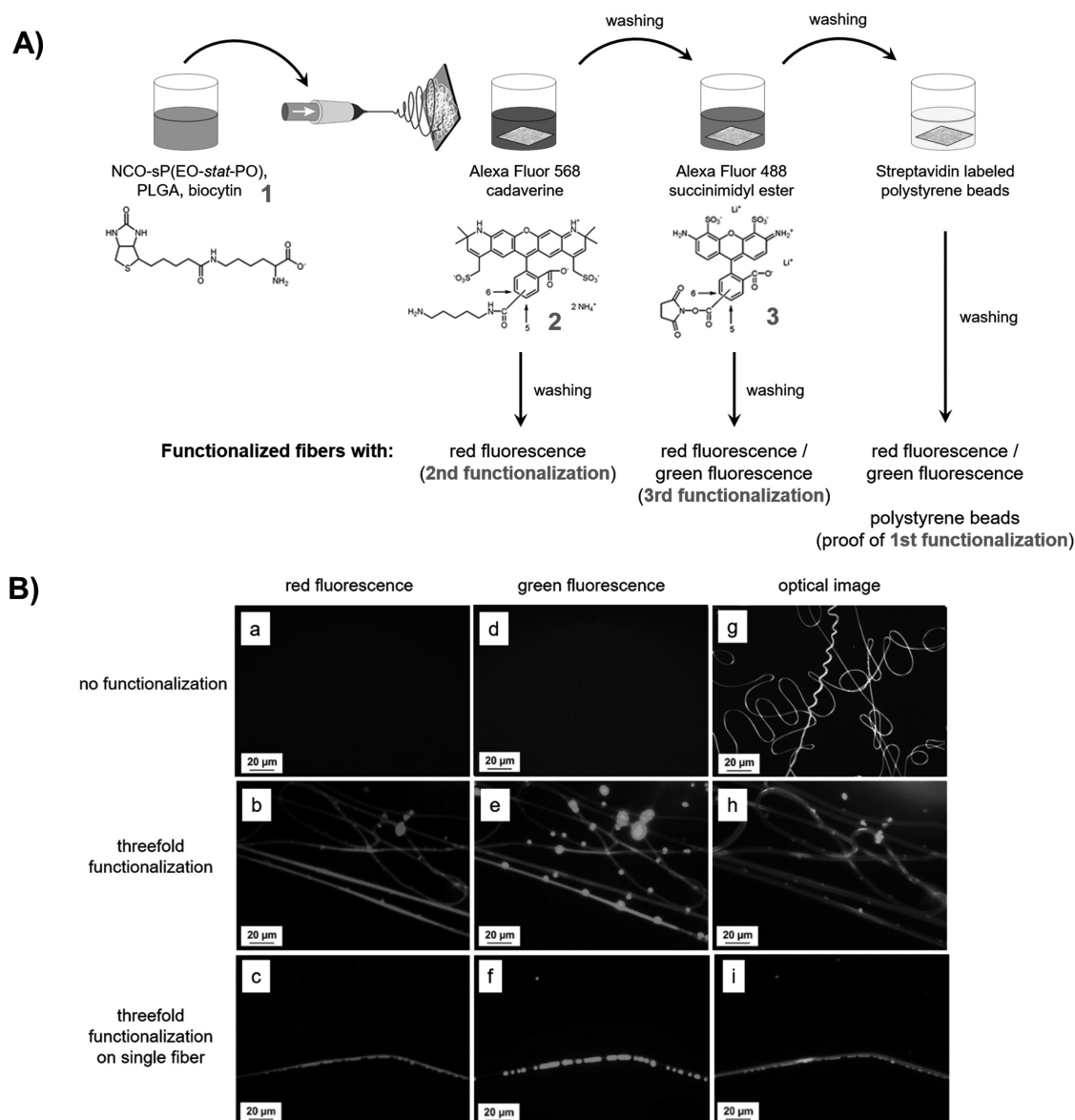


Figure 1. Threefold functionalization with biocytin and fluorescent dyes. A) Working protocol of immobilization of different components on electrospun fibers. First functionalization occurred by adding biocytin to the spinning solution; second functionalization was done by Alexa Fluor 568 cadaverine; third functionalization happened with Alexa Fluor 488 NHS ester. To demonstrate the success of the first functionalization, binding of SA beads was evaluated. B) Results of fluorescent staining. Top row: Control images of NCO-sP(EO-stat-PO)/PLGA fibers without any staining. Panels (a)–(c) represent the red and panels (d)–(f) the green fluorescence. Panels (g)–(i) show the optical images. The exposure time of panels (a) and (d) was 20 000 ms. Triple functionalization with Alexa Fluor 488 succinimidyl ester, Alexa Fluor 568 cadaverine, and SA-labeled polystyrene beads is shown in the middle and bottom row. The exposure time of panels (b) and (c) was 1000 ms. Panels (e) and (f) had an exposure time of 20 000 ms. In the bottom row, one single fiber is depicted to better show the fluorescence.

green fluorescence dye. The micrographs in the bottom row of Figure 1B have been taken from an area of the sample where less PS beads are bound and the weaker fluorescence of the fibers can be visualized more clearly.

2.2. Binding Assay with Biological Molecules

This robust threefold surface functionalization method for electrospun fibers can be exploited for a variety of applications. In

this study and in the context of biomaterials, we have focused on introducing several bioactive molecules to tune cell adhesion and the interaction with the immune system. As known from literature, the implantation of biomaterials could lead to immune reactions in vivo with inflammation and foreign body reactions.^[25] A modulation of such immune reactions would be beneficial to avoid an acute inflammation and material rejection and hence to improve the healing capacity of the scaffold. Inflammatory processes are commonly triggered by cytokines such as TNF or TWEAK.^[26] The former is a master cytokine

of the immune system which is expressed by macrophages and other cell types like mast cells to control different immune cells and tissue homeostasis.^[27] TWEAK and its receptor Fn14 induce the production of angiogenic and proinflammatory proteins or stimulate the proliferation and differentiation of progenitor cells to control tissue homeostasis and wound healing but the overshooting and chronic activities of these molecules are also strongly disease promoting in a variety of pathologies.^[28] Therefore, an immobilization of antagonists of the TNF/TNF receptor system and/or the TWEAK/Fn14 system on the electrospun fibers would be highly useful to control the foreign body reaction and to attenuate inflammation in tissue injury and remodeling by suppressing TNF- and/or TWEAK-induced pathways.^[18,29]

Initially, we investigated a functionalization protocol with a TNF-neutralizing antagonist (**Figure 2A**). For this issue, two antibodies were used: Rituximab, a human IgG1 antibody against the B-cell-specific cell-surface antigen CD20^[30] as negative control where no binding of TNF occurs, and Humira, a clinically used human IgG1 antibody against TNF.^[18] Humira inhibits TNF binding to its receptors TNFR1 and TNFR2 and was used here to evaluate the properties of antibody-modified fibers. To detect functional antibodies on the fiber, the protein GpL-FLAG-TNC-TNF was used; this construct consists of TNF with an N-terminal GpL-FLAG-TNC domain. GpL is the luciferase of *Gaussia princeps*; FLAG is a specific octapeptide

epitope exploited for purification and TNC is a short domain from tenascin-C used to stabilize the trimeric assembly of ligands of the TNF super family.^[31] The luciferase catalyzes the oxidation of the substrate coelenterazine to coelenteramide; this reaction results in the emission of light which could be linearly detected and measured over several orders of magnitude.

To demonstrate the functional immobilization of the TNF antibody on the isocyanate-decorated fibers, a binding assay was performed with a constant antibody-saturating concentration of GpL-FLAG-TNC-TNF and meshes that were incubated with increasing Humira concentrations immediately after spinning. In **Figure 2B**, it is shown that with higher concentrations of Humira used for immobilization more GpL-FLAG-TNC-TNF molecules bound to the fibers whereas surfaces modified with the control antibody Rituximab showed practically no GpL-FLAG-TNC-TNF binding. Rituximab served here for detecting the unspecific fiber binding of GpL-FLAG-TNC-TNF, which was very small. At lower Humira concentrations $<0.5 \text{ mg mL}^{-1}$, the increase of GpL-FLAG-TNC-TNF binding and thus the antibody immobilization was almost linear; with higher amounts of antibody of more than 2.5 mg mL^{-1} a saturation of binding sites was observed reflecting maximal immobilization of Humira. An additional modification was performed by immobilizing the peptide sequence CGRGDS^[32] on the fibers to offer binding anchors for cell attachment. Meshes with RGD modification showed lower

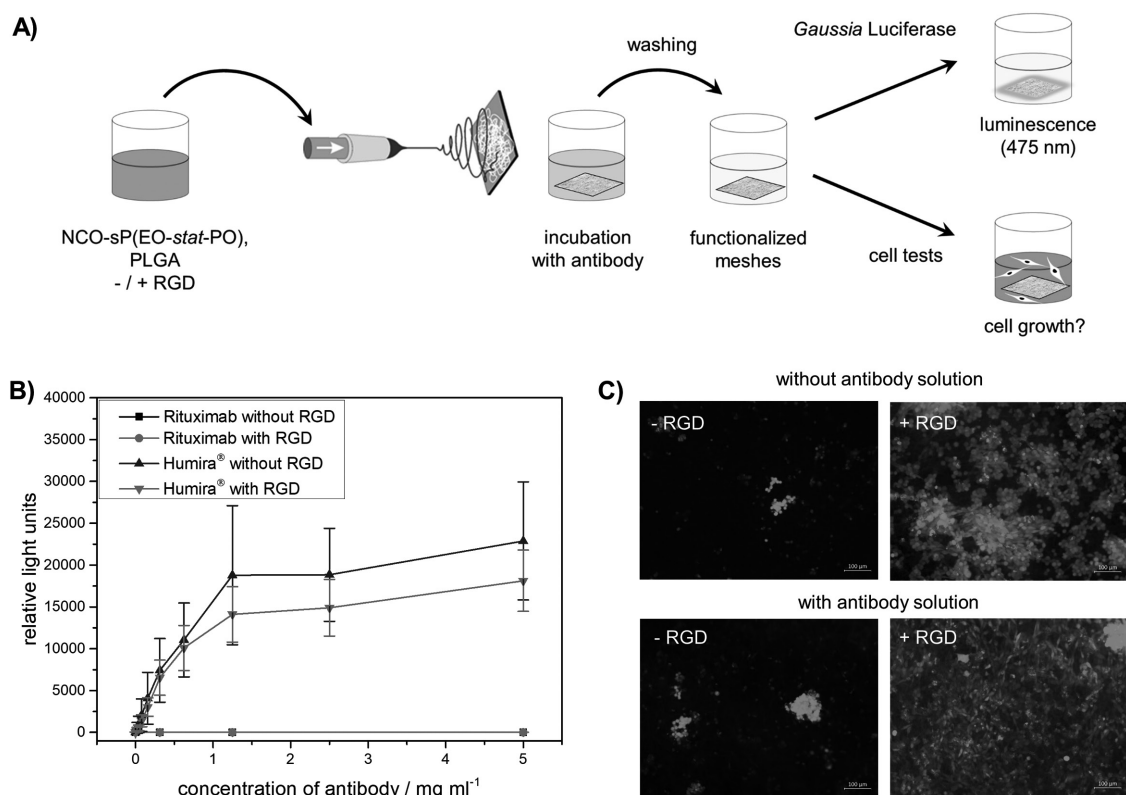


Figure 2. Biological functionalization of electrospun fibers. A) Functionalization protocol. B) Freshly spun meshes with and without RGD functionalization were incubated with indicated concentration of anti-CD20 Rituximab and anti-TNF Humira in PBS overnight at $4 \text{ }^{\circ}\text{C}$. After blockade of remaining reaction sites by treatment with serum supplemented with 10% FCS, meshes were incubated with 500 ng mL^{-1} GpL-FLAG-TNC-TNF. After removal of unbound molecules, mesh-bound GpL-FLAG-TNC-TNF molecules were quantified using BioLux Gaussia Luciferase Assay Kit ($n = 3$). C) L929 fibroblast growth on meshes \pm RGD functionalization and incubated with PBS (upper row) or with $350 \mu\text{g mL}^{-1}$ antibody solution (bottom row) ($n = 3$).

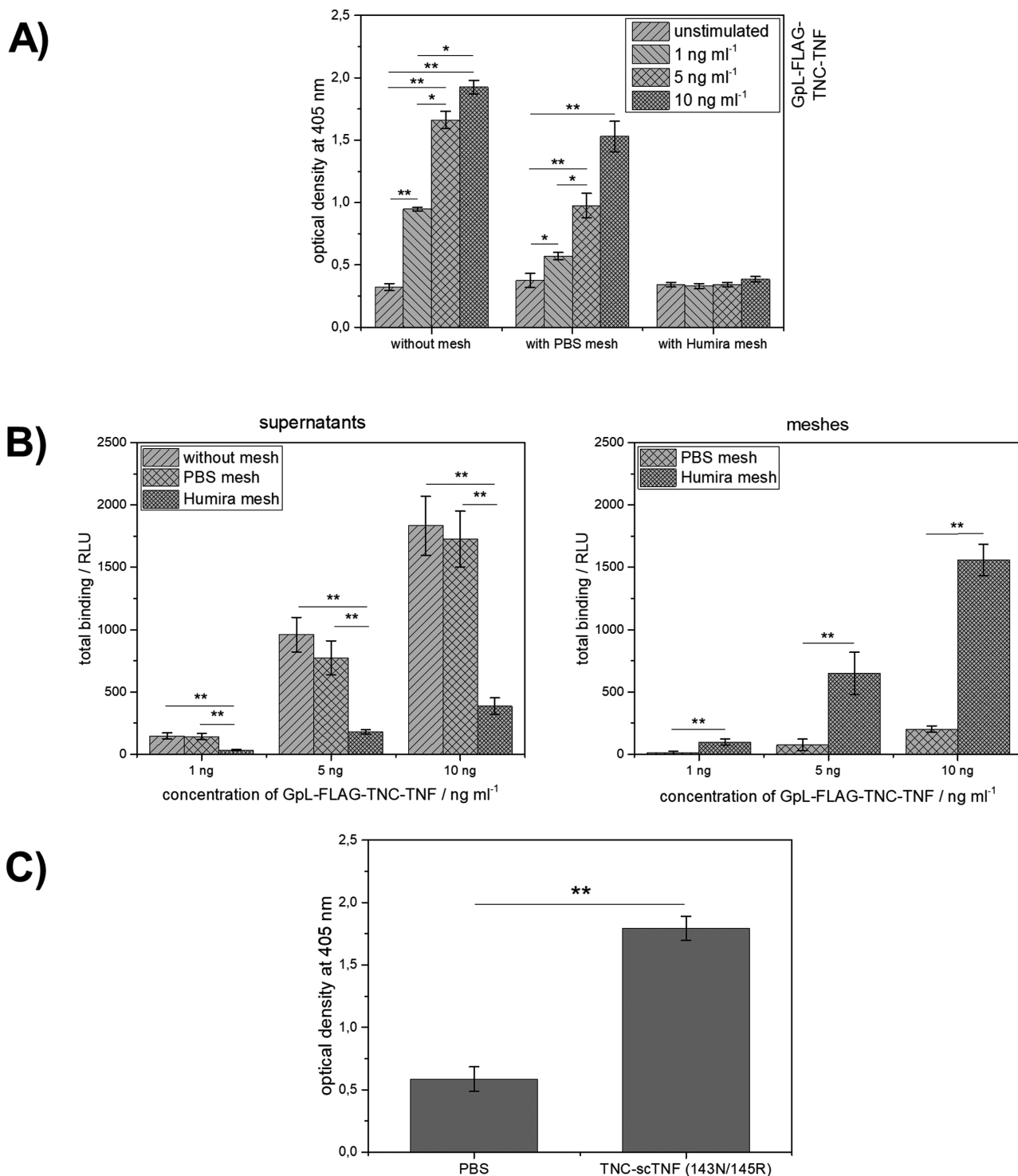


Figure 3. A) Inhibition of TNF activity by Humira functionalized electrospun meshes. Electrospun fibers treated with PBS or immobilized with Humira antibody were incubated with 200 μ L of 1, 5, or 10 ng mL⁻¹ GpL-FLAG-TNC-TNF solution in cell culture medium or in 200 μ L control medium. After 24 h, 100 μ L of the mesh supernatants were transferred to HT1080-Bcl2-TNFR2 cells and after overnight incubation, IL-8 production of the cells was measured by ELISA. Significant differences in IL-8 induction by supernatants of different GpL-FLAG-TNC-TNF concentrations for the same mesh type are shown. An additional experiment highlighting significant differences between different types of meshes at a given concentration of GpL-FLAG-TNC-TNF is shown in Figure S7 in the Supporting Information. Level of significance: *, $p < 0.05$; **, $p < 0.01$ ($n = 2$). B) TNF depletion by Humira-functionalized electrospun meshes. After incubating the meshes of (A) for 2 h in 200 μ L control medium or 200 μ L GpL-FLAG-TNC-TNF medium, GpL activity of an aliquot of 50 μ L was measured and multiplied with 4 to obtain total GpL activity of the supernatants (left side). Complementary, the GpL activity of the washed meshes was measured (right side). C) TNFR2 stimulatory activity of TNC-scTNF (143N/145R)-functionalized

GpL-FLAG-TNC-TNF binding than the meshes without RGD. Differences between the meshes without and with added peptide sequence were found to be significant at higher concentrations, which leads to the result that some binding sites potentially accessible for Humira immobilization have been blocked by the previous immobilization of RGD peptide.

In a further approach, cells were seeded onto the fibers to study whether the immobilized antibody interferes with cell growth on RGD-functionalized meshes. L929 mouse fibroblasts were seeded on RGD meshes over 4 d at 37 °C to compare different surface modifications (Figure 2C). As positive control, a pure PLGA mesh was used which was electrospun without addition of NCO-sP(EO-*stat*-PO) to create a hydrophobic surface with unspecific protein adsorption and strong cell adherence (Figure S5, Supporting Information). Meshes without immobilized antibody almost inhibited fibroblast growth; the same result was found for the mesh with immobilized Humira in a concentration of 350 µg mL⁻¹. After introducing RGD on the fiber surface, fibroblast growth was strongly enhanced irrespective whether the mesh has been incubated with phosphate buffered saline (PBS) or antibody solution, leading to the conclusion that cell proliferation on RGD meshes was not essentially influenced by the second functionalization with antibody. This was also shown by fixation of cells and visualization with a scanning electron microscope (SEM) (Figure S6, Supporting Information) where L929 fibroblasts adhered well on both fiber surfaces.

2.3. Enzyme-Linked Immunosorbent Assay (ELISA)

In the second functionalization step with Humira, a surface was prepared which could dampen proinflammatory immune reactions in the body by depletion of TNF by immobilized Humira on fiber meshes. To evaluate this possibility, GpL-FLAG-TNC-TNF-supplemented cell culture medium was added to meshes with immobilized Humira and was used 2 h later to stimulate HT1080-Bcl2-TNFR2 cells, a variant of the HT1080 colon carcinoma cell line,^[33] which produces IL-8 in response to TNF receptor stimulation.^[34]

A corresponding ELISA evaluation of IL-8 production is shown in Figure 3A. Supernatants of control meshes without antibody immobilization and cell culture medium containing GpL-FLAG-TNC-TNF without mesh contact showed the same amount of IL-8 production. However, when HT1080-Bcl2-TNFR2 cells were challenged with supernatants of meshes functionalized with Humira, they showed a significantly decreased IL-8 production, which indicates TNF depletion by the mesh and thus an antiinflammatory effect of the functionalized fibers. To directly verify depletion of GpL-FLAG-TNC-TNF, both the GpL activities bound to the meshes and from the corresponding cell culture supernatants used for cell stimulation were determined. In accordance with the strong inhibitory effect of the Humira-functionalized mesh on the ability of GpL-FLAG-TNC-TNF containing supernatants to trigger IL-8

production (Figure 3A), there was a near-to-complete specific binding of GpL-FLAG-TNC-TNF to the Humira meshes and thus complementary an efficient depletion of this proinflammatory cytokine from the supernatant (Figure 3B).

To evaluate whether PLGA meshes electrospun with NCO-sP(EO-*stat*-PO) cannot only be functionalized with antibodies but also with other types of proteins, we used as a model TNC-scTNF (143N/145R), a trimeric fusion protein of single-chain TNF^[35] with changed amino acids on positions 143 and 145 of TNF which only binds to TNFR2 and which in vivo does not trigger a life-threatening TNFR1-dependent cytokine storm.^[36] Freshly electrospun RGD-modified meshes were incubated with TNC-scTNF (143N/145R) solution for a second functionalization on the fiber surface and were colonized after removal of unbound TNC-scTNF (143N/145R) molecules with HT1080-Bcl2-TNFR2 cells. To detect the presence of functional immobilized TNC-scTNF (143N/145R) molecules on the meshes, supernatants were analyzed after overnight incubation at 37 °C concerning the production of IL-8, which is induced in HT1080-Bcl2-TNFR2 cells by stimulation of each of the two TNF receptors. As it is evident from Figure 3C, there was a significant difference between meshes, which were treated as a control with PBS, and those which were immobilized with TNC-scTNF (143N/145R). From these results, it could be concluded that the cells not only can survive on the meshes but also are able to respond to cytokine molecules immobilized on these meshes. Additionally, to show the good adherence of HT1080-Bcl2-TNFR2 on electrospun RGD meshes independently of immobilized molecules, SEM examination was performed (Figure S6, Supporting Information).

2.4. Twofold and Threefold Functionalization

Next, we examined if there is a reciprocal influence between different antibodies when simultaneously immobilized on the electrospun mesh (Figure 4A). Three different antibodies were used: Rituximab as negative control; Humira whose functionality can be tested as described before by binding of GpL-FLAG-TNC-TNF and 5B6, an Fn14-specific antibody, which can be detected by its ability to bind Fn14(ed)-TNC-FLAG-GpL, a recombinantly produced luciferase fusion protein of Fn14 containing the extracellular domain of this receptor.^[19] As shown in Figure 4B, there is hardly any difference between the binding of GpL-FLAG-TNC-TNF and Fn14(ed)-TNC-FLAG-GpL to meshes functionalized with Humira and 5B6. This led to the conclusion that both antibodies were immobilized on the mesh with the same amount demonstrating a successful twofold functionalization in one step on the fiber surface. A threefold functionalization with the same antibody mixture was obtained by adding RGD to the spinning solution. Also on these meshes, the amount of immobilized proteins was practically the same for both model antibodies. When comparing the values of the meshes without RGD and with RGD, the relative light units for RGD meshes are significantly lower than

electrospun meshes. Electrospun fibers were treated with PBS or immobilized with TNC-scTNF (143N/145R). After washing, meshes were transferred in 100 µL medium to HT1080-Bcl2-TNFR2 cells and after overnight incubation, IL-8 production of the cells was measured by ELISA. Level of significance: **, $p < 0.01$ ($n = 3$).

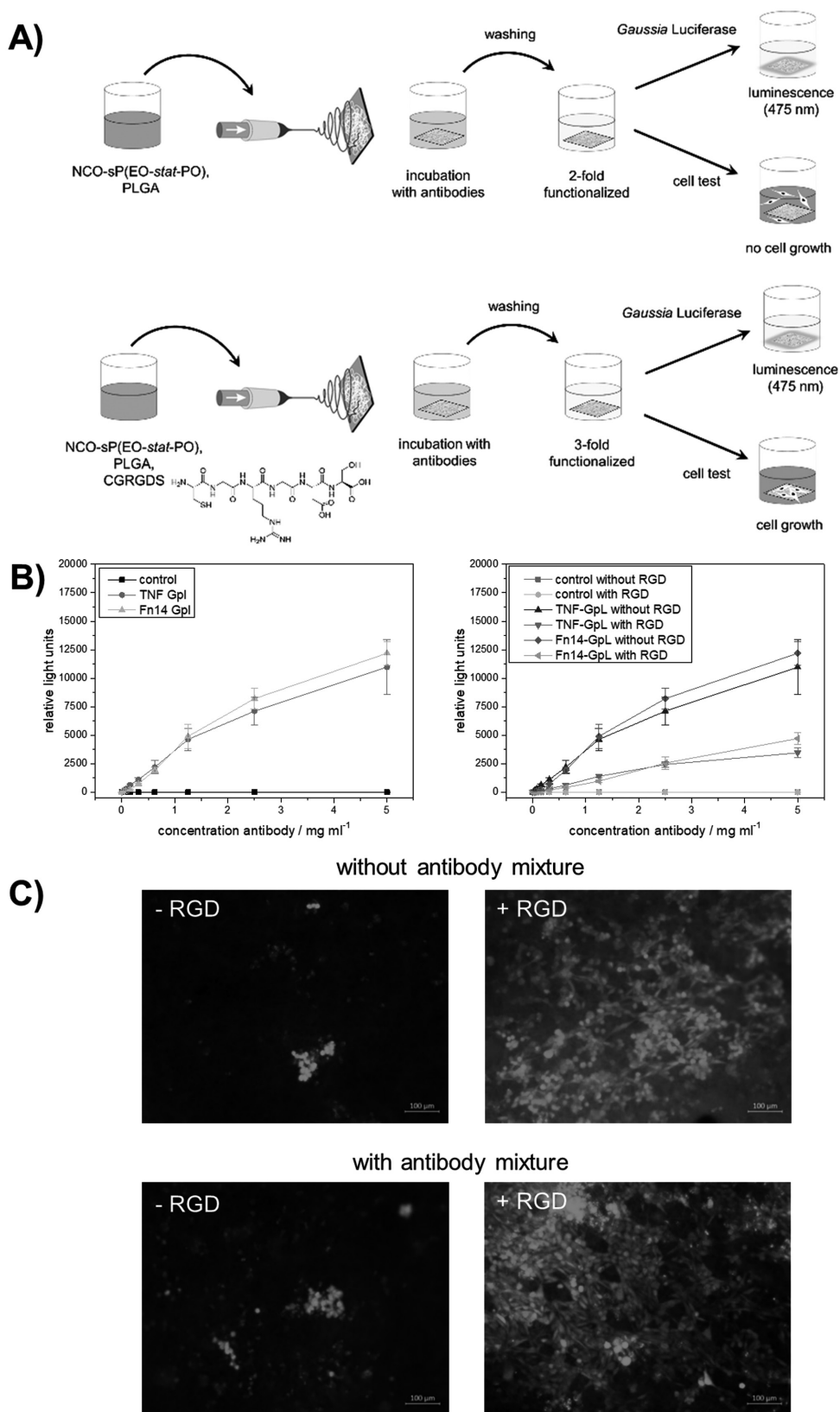


Figure 4. Two- and threefold biological functionalization. A) Functionalization protocol. Upper row: Twofold functionalization. Bottom row: Threefold functionalization. B) Antigen binding curve of meshes with immobilized antibodies without (left side) and with (right side) RGD prefunctionalization. The \pm RGD scaffolds were incubated with the indicated concentration of an equimolar antibody mixture of Humira and 5B6. Immobilized functional

the values of meshes without RGD. This phenomenon can be explained again by the fact that less binding sites are available on the mesh for antibody binding because RGD blocks a fraction of the free isocyanate groups free isocyanate groups already during electrospinning.

For cell experiments, it was expected that L929 fibroblasts would grow on RGD-functionalized and not on the unfunctionalized meshes because of their hydrophilicity. In Figure 4C, the difference between meshes without and with RGD is noticeable. In addition, meshes which were incubated with the antibody mixture composed of Humira and 5B6 showed a similar behavior to meshes which are only incubated with PBS. This supports the hypothesis that there is no influence of the immobilized antibodies on cell growth of L929 and HT1080–Bcl–TNFR2 cells.

3. Conclusion

This study introduces a robust chemical crosslinker free method to covalently surface functionalize electrospun fiber meshes. The method was demonstrated with fluorescent dyes and then used to decorate fiber surfaces with the cell-adhesion-mediating peptide sequence RGD and at the same time with one or two antibodies. Thus, with prefunctionalized RGD meshes, the use of mixtures of two different antibodies allows a threefold functionalization in two steps. Both fibroblast and HT1080 cell growth were possible on such functionalized fibers, but only when RGD functional fibers were used; without the peptides, the cells could not adhere to the fibers. HT1080 cells were demonstrated to interact with immobilized proteins only in the presence of RGD peptides when they are able to adhere, and IL-8 production could be altered. With the demonstrated effect on IL-8 production of adherent cells, we envision that corresponding meshes could be used as immunomodulatory wound dressing materials.

4. Experimental Section

Electrospinning: NCO–sP(EO-*stat*-PO) (DWI Leibniz-Institute for Interactive Materials, Aachen, Germany) was dissolved in dry dimethyl sulfoxide (DMSO) and stirred for 10 min. The solution was diluted with acetone (DMSO–acetone ratio 1:5 V/V), briefly mixed, and finally PLGA (Resomer RG504, Evonik, Essen, Germany) was added and stirred until the solution was homogenous. The polymer content of the solution was 5 wt% for NCO–sP(EO-*stat*-PO) and 24.5 wt% for PLGA. Polymer mixtures were fed at 0.5 mL h⁻¹ through a flat-tip stainless steel spinneret connected to a high-voltage power supply, and a high voltage of 13 kV was applied to the spinning solution. The collection distance between spinneret and target was 15 cm. The nonwoven meshes were collected on a rotating drum as grounded collector (diameter 60 mm, length 100 mm) with a rotation speed of 120 rpm. For cell experiments, fibers were produced with 0.09 wt% CGRGDS (jpt Peptide Technologies GmbH, Berlin, Germany). Therefore, the peptide was dissolved in DMSO before solving of the NCO–sP(EO-*stat*-PO).

Consecutive Functionalization: Electrospun fibers on glass coverslips coated with NCO–sP(EO-*stat*-PO) as described before^[19] were incubated 5 min after electrospinning with Alexa Fluor 568 cadaverine (0.05 mg mL⁻¹; Life technologies, Germany) in water for 15 min. After rinsing three times with deionized water, the samples were incubated with Alexa Fluor 488 succinimidyl ester (0.05 mg mL⁻¹; Life technologies, Germany) in water for 2 h. After a second thorough rinsing with deionized water, SA microspheres with a diameter of 1.0 μm (Polysciences Europe GmbH, Eppelheim, Germany) were bound specifically onto the fibers. Therefore, the fibers were immersed in SA-labeled latex beads (20 μL) labeled with fluorescein isocyanate for easier visualization purposes and diluted with deionized water (980 μL) for 60 min. The samples were rinsed thoroughly with deionized water and dried in a stream of nitrogen. The functionalized samples were examined with fluorescence and optical microscopy using a Zeiss Stemi 2000-C (Jena, Germany).

Incubation with Antibodies and Proteins: Freshly spun meshes were cut into 1 × 1 cm pieces and incubated with different antibodies or antibody mixtures in PBS overnight at 4 °C while shaking. Humira (Adalimumab; AbbVie, Wiesbaden, Germany), and MabThera (Rituximab; Roche, Basel, Switzerland), were kindly provided from the University Hospital of Würzburg and the Fn14-specific antibody 5B6 had been produced and purified as described elsewhere.^[19] Remaining solution was removed and the samples were incubated with RPMI1640 medium (PAA, Pasching, Germany) supplemented with 10% fetal calf serum (FCS) for 1.5 h to stop the reaction and to block the remaining binding sites. The meshes were washed five times with PBS and subsequently incubated for 1 h with *G. princeps* luciferase (GpL) fusion proteins of TNF (GpL–FLAG–TNC–TNF)^[31] or Fn14 (Fn14(ed)–TNC–FLAG–GpL). The binding of the GpL fusion proteins was used to indirectly detect and quantify functional antibody molecules. After repeated washing with PBS, each sample was cut into four pieces and transferred into a UV 96-well plate (Greiner FLUOTRAC 200 96-well plates black medium binding), and GpL activity was determined using a Gaussia Luciferase Assay Kit (BioLux, New England Biolabs GmbH, Frankfurt am Main, Germany) and a Luminometer (Lucy 2, Anthos Labtec Instruments, Wals/Salzburg, Austria). As a minor modification, in the experiments where low physiological relevant concentrations of TNF have been used (Figure 3A,B), the control meshes were incubated after the FCS block for 1 h with Humira solution to absolutely assure that differences in the TNF-inhibitory effect between PBS and Humira meshes are due to immobilized Humira and not affected by microtraces of unspecifically bound Humira resisting washing.

Cell Culture: For the fibroblast tests, L929 murine fibroblasts were seeded in a 24-well tissue culture plate (50 000 cells per well in 1 mL DMEM plus 10% FCS, 1% penicillin/streptomycin) onto the meshes with RGD modification. Fiber mats were fixed in the culture plates using cell crowns (MINUCELLS and MINUTISSUE, Bad Abbach, Germany) at a distance of 1.25 mm from the bottom. The cells were incubated for 4 d at 37 °C in a 5% CO₂-humidified atmosphere. To analyze growth of L929 cells on functionalized meshes, a live/dead staining was accomplished after incubation. Living cells were fluorescently colored in green by calcein AM (Life technologies, Germany) and dead cells in red by ethidium homodimer-1 (Sigma Aldrich, Germany). Fluorescence images were taken with the Axio Imager M1 (Carl Zeiss, Germany). For further examination of cell adhesion and morphology, meshes with cells were fixed and dried and an SEM (FIB-SEM-microscope CB 340, Carl Zeiss, Jena, Germany) was used.

IL-8 ELISA: Supernatants were collected and analyzed for their IL-8 content using a commercially available ELISA kit (BD OptEIA, BD Biosciences, San Diego, CA) according to the manufacturer's instructions.

antibodies were selectively quantified using either binding of 500 ng mL⁻¹ GpL–FLAG–TNC–TNF or 500 ng mL⁻¹ Fn14(ed)–TNC–FLAG–GpL ($n = 2$). C) L929 fibroblast growth on meshes ±RGD functionalization and incubated with PBS (upper row) and with antibody mixture of Humira and 5B6 (bottom row) ($n = 3$).

Analysis of Variance (ANOVA): ANOVA was examined by means of SigmaPlot (Systat Software GmbH, Erkrath, Germany) using 1-way or 2-way ANOVA depending on the raw data. In order to calculate the statistical significance, a post hoc Tukey test was performed.

Supporting Information

Supporting Information is available from the Wiley Online Library or from the author.

Acknowledgements

This research was funded by the European Research Council under grant agreement 617989 (Design2Heal). The authors gratefully acknowledge the DFG State Major Instrumentation Programme, funding the crossbeam scanning electron microscope Zeiss CB 340 (INST 105022/58-1 FUGG), and also thank Philipp Stahlhut for assistance with the SEM images.

Conflict of Interest

The authors declare no conflict of interest.

Keywords

antibodies, electrospinning, immune response, nanofibers, surface functionalization

Received: May 30, 2017
Revised: August 22, 2017
Published online:

- [1] J. Doshi, D. H. Reneker, *J. Electrostat.* **1995**, 35, 151.
[2] M. Hajra, K. Mehta, G. Chase, *Sep. Purif. Technol.* **2003**, 30, 79.
[3] S. Ji, Y. Li, M. Yang, *Sens. Actuators, B* **2008**, 133, 644.
[4] K. Pawlowski, H. Belvin, D. Raney, J. Su, J. Harrison, E. Siochi, *Polymer* **2003**, 44, 1309.
[5] a) T. J. Sill, H. A. von Recum, *Biomaterials* **2008**, 29, 1989; b) S. Sell, C. Barnes, M. Smith, M. McClure, P. Madurantakam, J. Grant, M. McManus, G. Bowlin, *Polym. Int.* **2007**, 56, 1349.
[6] Q. P. Pham, U. Sharma, A. G. Mikos, *Tissue Eng.* **2006**, 12, 1197.
[7] a) S. Agarwal, A. Greiner, J. H. Wendorff, *Adv. Funct. Mater.* **2009**, 19, 2863; b) W. J. Li, C. T. Laurencin, E. J. Caterson, R. S. Tuan, F. K. Ko, *J. Biomed. Mater. Res.* **2002**, 60, 613.
[8] J. S. Tjia, B. J. Aneskievich, P. V. Moghe, *Biomaterials* **1999**, 20, 2223.
[9] H. S. Yoo, T. G. Kim, T. G. Park, *Adv. Drug Delivery Rev.* **2009**, 61, 1033.
[10] a) S. Turmanova, M. Minchev, K. Vassilev, G. Danev, *J. Polym. Res.* **2008**, 15, 309; b) M. Mori, Y. Uyama, Y. Ikada, *J. Polym. Sci., Part A: Polym. Chem.* **1994**, 32, 1683; c) R.-Q. Kou, Z.-K. Xu, H.-T. Deng, Z.-M. Liu, P. Seta, Y. Xu, *Langmuir* **2003**, 19, 6869; d) Z. Ma, M. Kotaki, T. Yong, W. He, S. Ramakrishna, *Biomaterials* **2005**, 26, 2527.
[11] M. B. Taskin, R. Xu, H. Gregersen, J. V. Nygaard, F. Besenbacher, M. Chen, *ACS Appl. Mater. Interfaces* **2016**, 8, 15864.
[12] A. M. Nicolini, T. D. Toth, J.-Y. Yoon, *Colloids Surf., B* **2016**, 145, 830.
[13] P. Viswanathan, E. Themistou, K. Ngamkham, G. C. Reilly, S. P. Armes, G. Battaglia, *Biomacromolecules* **2014**, 16, 66.
[14] a) D. Grafahrend, K.-H. Heffels, M. V. Beer, P. Gasteier, M. Möller, G. Boehm, P. D. Dalton, J. Groll, *Nat. Mater.* **2011**, 10, 67; b) A. Rossi, L. Wistlich, K.-H. Heffels, H. Walles, J. Groll, *Adv. Healthcare Mater.* **2016**, 5, 1939; c) P. Gasteier, A. Reska, P. Schulte, J. Salber, A. Offenhäusser, M. Moeller, J. Groll, *Macromol. Biosci.* **2007**, 7, 1010.
[15] a) A. Vishwakarma, N. S. Bhise, M. B. Evangelista, J. Rouwkema, M. R. Dokmeci, A. M. Ghaemmaghami, N. E. Vrana, A. Khademhosseini, *Trends Biotechnol.* **2016**, 34, 470; b) R. Sridharan, A. R. Cameron, D. J. Kelly, C. J. Kearney, F. J. O'Brien, *Mater. Today* **2015**, 18, 313.
[16] a) E. M. Sussman, M. C. Halpin, J. Muster, R. T. Moon, B. D. Ratner, *Ann. Biomed. Eng.* **2014**, 42, 1508; b) M. Bartneck, K.-H. Heffels, Y. Pan, M. Bovi, G. Zwadlo-Klarwasser, J. Groll, *Biomaterials* **2012**, 33, 4136.
[17] S. Franz, S. Rammelt, D. Scharnweber, J. C. Simon, *Biomaterials* **2011**, 32, 6692.
[18] R. E. Kontermann, P. Scheurich, K. Pfizenmaier, *Expert Opin. Drug Discovery* **2009**, 4, 279.
[19] J. Trebing, I. Lang, M. Chopra, S. Salzmann, M. Moshir, K. Silence, S. S. Riedel, D. Siegmund, A. Beilhack, C. Otto, *mAbs* **2014**, 6, 297.
[20] A. Lancuški, F. Bossard, S. Fort, *Biomacromolecules* **2013**, 14, 1877.
[21] a) D. Grafahrend, K. H. Heffels, M. Möller, D. Klee, J. Groll, *Macromol. Biosci.* **2010**, 10, 1022; b) H. Cho, S. K. Madhurakkt Perikamana, J. Lee, J. Lee, K. Lee, C. S. Shin, H. Shin, *ACS Appl. Mater. Interfaces* **2014**, 6, 11225.
[22] X. Y. Sun, R. Shankar, H. G. Börner, T. K. Ghosh, R. J. Spontak, *Adv. Mater.* **2007**, 19, 87.
[23] P. C. Weber, D. Ohlendorf, J. Wendoloski, F. Salemme, *Science* **1989**, 243, 85.
[24] J. Groll, M. Moeller, *Methods Enzymol.* **2010**, 472, 1.
[25] a) J. M. Anderson, *Annu. Rev. Mater. Res.* **2001**, 31, 81; b) B. D. Ratner, S. J. Bryant, *Annu. Rev. Biomed. Eng.* **2004**, 6, 41.
[26] a) L. A. Tartaglia, D. V. Goeddel, *Immunol. Today* **1992**, 13, 151; b) S. R. Wiley, J. A. Winkles, *Cytokine Growth Factor Rev.* **2003**, 14, 241.
[27] G. Chen, D. V. Goeddel, *Science* **2002**, 296, 1634.
[28] H. Wajant, *Br. J. Pharmacol.* **2013**, 170, 748.
[29] a) S. Thangaraju, E. Subramani, B. Chakravarty, K. Chaudhury, *Gynecol. Oncol.* **2012**, 127, 426; b) L. C. Burkly, J. S. Michaelson, T. S. Zheng, *Immunol. Rev.* **2011**, 244, 99; c) L. C. Burkly, *Semin. Immunol.* **2014**, 26, 229.
[30] K. L. Everton, D. R. Abbott, D. K. Crockett, K. S. Elenitoba-Johnson, M. S. Lim, *J. Chromatogr. B* **2009**, 877, 1335.
[31] A. Fick, I. Lang, V. Schäfer, A. Seher, J. Trebing, D. Weisenberger, H. Wajant, *J. Biol. Chem.* **2012**, 287, 484.
[32] V. A. Schulte, K. Hahn, A. Dhanasingh, K.-H. Heffels, J. Groll, *Biofabrication* **2014**, 6, 024106.
[33] D. F. Legler, O. Micheau, M.-A. Doucey, J. Tschopp, C. Bron, *Immunity* **2003**, 18, 655.
[34] Y. Wu, B. Zhou, *Br. J. Cancer* **2010**, 102, 639.
[35] A. Krippner-Heidenreich, I. Grunwald, G. Zimmermann, M. Kühnle, J. Gerspach, T. Sterns, S. D. Shnyder, J. H. Gill, D. N. Männel, K. Pfizenmaier, *J. Immunol.* **2008**, 180, 8176.
[36] H. Rauert, A. Wicovsky, N. Müller, D. Siegmund, V. Spindler, J. Waschke, C. Kneitz, H. Wajant, *J. Biol. Chem.* **2010**, 285, 7394.